

## Enhancing friction and wear performance in hybrid aluminum composites through grey relational analysis

Dinesh Kumar, Satnam Singh

Online Publication Date: 08 January 2024

URL: <http://www.jresm.org/archive/resm2024.05ma1012tn.html>

DOI: <http://dx.doi.org/10.17515/resm2024.05ma1012tn>

Journal Abbreviation: *Res. Eng. Struct. Mater.*

### To cite this article

Kumar D, Singh S. Enhancing friction and wear performance in hybrid aluminum composites through grey relational analysis. *Res. Eng. Struct. Mater.*, 2024; 10(3): 943-956.

### Disclaimer

All the opinions and statements expressed in the papers are on the responsibility of author(s) and are not to be regarded as those of the journal of Research on Engineering Structures and Materials (RESM) organization or related parties. The publishers make no warranty, explicit or implied, or make any representation with respect to the contents of any article will be complete or accurate or up to date. The accuracy of any instructions, equations, or other information should be independently verified. The publisher and related parties shall not be liable for any loss, actions, claims, proceedings, demand or costs or damages whatsoever or howsoever caused arising directly or indirectly in connection with use of the information given in the journal or related means.



Published articles are freely available to users under the terms of Creative Commons Attribution - NonCommercial 4.0 International Public License, as currently displayed at [here](#) (the "CC BY - NC").

## Enhancing friction and wear performance in hybrid aluminum composites through grey relational analysis

Dinesh Kumar<sup>\*,a</sup>, Satnam Singh<sup>b</sup>

Department of Mechanical Engineering, National Institute of Technology Kurukshetra, India

### Article Info

### Abstract

#### Article history:

Received 12 Oct 2023  
Accepted 08 Jan 2024

#### Keywords:

Al-6061 alloy;  
Graphene;  
Silicon carbide;  
Hardness;  
Tensile strength;  
Friction;  
Wear;  
GRA

Hybrid aluminum metal matrix composites (AMMCs) include qualities including being lightweight, very effective, and highly resistant to wear, and corrosion. The process used in this study to maximize friction and minimize wear of hybrid AMMCs involves applying grey relational analysis (GRA) to optimize the process features. Stir-casting was used to create hybrid AMMCs of the Al-6061 alloy reinforced with graphene (Gr) and silicon carbide (SiC). The experiment used Taguchi's  $L_{27}$  design, and three process parameters—normal load, sliding distance, and sliding speed—were combined with GRA to produce the maximum coefficient of friction and lowest wear rate. Al-6Gr-6SiC obtained the maximum hardness of 128 VHN and 253 MPa as tensile strength, further coefficient of friction, and wear were analyzed for the same composite., respectively. The ideal mixture of graphene (6 weight percent) and silicon carbide (6 weight percent) as reinforcement in Al-6061 alloy obtained the optimum value of frictional coefficient (0.29766) and wear (0.002588 mm<sup>3</sup>/m), respectively.

© 2024 MIM Research Group. All rights reserved.

## 1. Introduction

Aluminum alloys are extensively used as matrix materials in producing metal matrix composites (MMCs). These composites use the advantageous qualities of aluminum alloys while integrating reinforcing elements to attain improved mechanical, thermal, or other distinct performance characteristics. Due to their higher mechanical qualities compared to monolithic materials, aluminum alloys are deemed to be the most appropriate materials in the aerospace and automotive sectors. Aluminum alloys are popular among researchers for the creation of novel materials with improved properties because of their affordability and ease of supply [1]. A composite is a multi-stage construction that is created by combining reinforcements and a matrix. When metal is employed as the matrix material during the production process, the created composite is referred to as a Metal Matrix Composite (MMC) [2]. Aluminum alloys and two or more reinforcements are combined to create hybrid aluminum metal matrix composites (AMMCs), which have exceptional mechanical and tribological qualities [3]. Due to its high magnesium and silicon content, the aluminum alloy 6XXX series has already been utilized in the transportation and automotive industries. Due to its castability, the Al-6061 alloy is discovered to be the most popular alloy in the 6XXX family. Al-6061 alloy is used to make lightweight automobile components as well [4]. Al-6061 was used as the matrix in the current experiment, with Gr and SiC particles serving as reinforcement. Using Taguchi's  $L_{27}$  experimental design, the friction and wear of manufactured AMMCs were measured under ASTM standards [5]. The ideal set of process parameters at which the friction and wear values reach their optimum

\*Corresponding author: [dinesh.61900120@nitkkr.ac.in](mailto:dinesh.61900120@nitkkr.ac.in)

<sup>a</sup> orcid.org/0000-0003-1885-2431; <sup>b</sup> orcid.org/0000-0002-5648-6113

DOI: <http://dx.doi.org/10.17515/resm2024.05ma1012tn>

Res. Eng. Struct. Mat. Vol. 10 Iss. 3 (2024) 943-956

levels was found using the GRA approach [6]. A hybrid composite was formed by including graphene (Gr) and silicon carbide (SiC) as dual reinforcements in the aluminum matrix. The present literature has yet to extensively investigate the combination of graphene (Gr) and silicon carbide (SiC). Research publications often demonstrate the use of either SiC or graphene as a sole reinforcement or in combination with other reinforcements such as Al<sub>2</sub>O<sub>3</sub>, CNT, TiC, etc. [7]–[11]. The limited availability of literature on the particular combination of silicon carbide and graphene highlights our work's originality and unique character, enhancing the overall comprehension of hybrid composites with the capacity to reveal new synergies between these two reinforcing elements. The amount of reinforcement can be used up to 20% in metal matrix composites to avoid negative effects on the mechanical properties of the composite. Excessive amounts of reinforcement material can lead to poor bonding between the reinforcement and matrix, resulting in reduced ductility and toughness. The decision to restrict the experimentation to 12% for (6% graphene and 6% silicon carbide) despite the observed increase in hardness with higher percentages of these reinforcements may be attributed to several factors. While higher hardness is generally preferred for improved wear performance in certain applications, such as Parts like pistons, cylinder liners, and connecting rods will benefit from improved hardness and wear resistance. While higher percentages of reinforcement materials beyond 12% lead to agglomeration of the reinforcement particles.

## 2. Materials and Methods

### 2.1. Materials Used

In this investigation, Al-6061 alloy is used as the matrix or base alloy and its composition is shown in Table 1. Figure 1 shows the EDAX analysis of Al-6061 alloy that gives the elemental composition of the material. The graphene and silicon carbides are used as reinforcements and their properties are mentioned in Table 2.

Table 1. Matrix material composition

|          |          |           |          |           |      |
|----------|----------|-----------|----------|-----------|------|
| Elements | Aluminum | Magnesium | Silicon  | Copper    | Iron |
| Wt. %    | 97.2     | 1.00      | 0.6      | 0.25      | 0.40 |
| Elements | Chromium | Zinc      | Titanium | Manganese |      |
| Wt. %    | 0.195    | 0.125     | 0.125    | 0.080     |      |

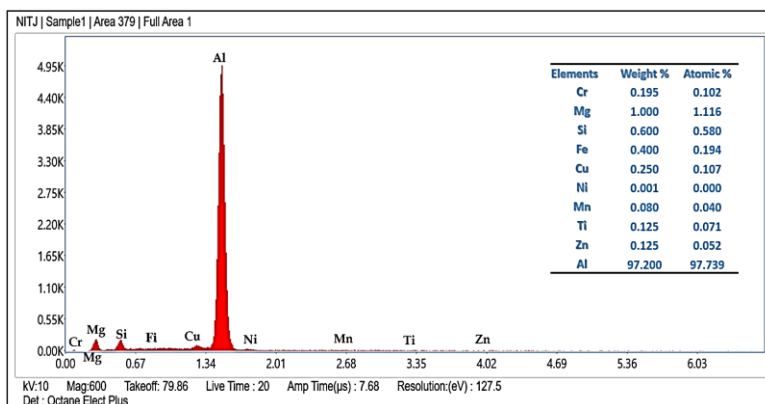


Fig. 1. EDAX analysis of Al-6061 alloy

Table 2. Reinforcement particle specifications

| Reinforcement | Melting Point (°C) | Particle size | Density (g/cm <sup>3</sup> ) |
|---------------|--------------------|---------------|------------------------------|
| Gr- Powder    | 3650               | 5 nm          | 2.30                         |
| SiC- Powder   | 2700               | 220 μm        | 3.20                         |

## 2.2. Methodology

### 2.2.1 Fabrication of Hybrid Composite

The manufacture of MMCs may be done using several different methods, most of which can be divided into liquid-state and solid-state methods [6]. In this study, Gr and SiC particles were used as reinforcements while Al-6061 was used as the matrix to create the hybrid AMMCs. With the use of a high-frequency induction heater, solid metal is first heated to 750°C in a graphite crucible until it melts or becomes semi-solid [12]. The reinforcements (graphene and silicon carbide) were then applied to the molten metal matrix after preheating. Figure 2 (a) shows the experimental setup of the stir-casting process and Figure 2 (b) shows the fabricated samples.



Fig. 2. Experimental setup and fabricated samples

To achieve the homogeneous mixing of reinforcements into the molten matrix material, a graphite stirrer was employed. Mg and Zr are utilized in quantities of 2wt% for improved reinforcement wettability in the matrix [13]. Tetrachloroethane degasser is used to take carbon dioxide, nitrogen, and hydrogen out of the aluminum melt. To avoid melt oxidation, the entire procedure is carried out under an environment of inert gas, namely Argon. The melt is poured into the die, let to harden, and then removed to be processed further. The nomenclature of fabricated samples is mentioned in Table 3.

Table 3. Nomenclature of fabricated hybrid composites

| S. No | Material    | Composition              |
|-------|-------------|--------------------------|
| 1     | Al-6Gr-4SiC | 90% Al + 6% Gr + 4% SiC  |
| 2     | Al-4Gr-6SiC | 90% Al + 4% Gr + 6% SiC  |
| 3     | Al-6Gr-6SiC | 88% Al + 6% Gr + 6 % SiC |

### 2.2.2 Dry Sliding Wear

According to the ASTM G99 standard, the samples' wear behavior was examined using pin-on-disc wear test equipment [14]. The counter plate was constructed using EN31 steel,

which has a hardness of 62 HRC. The revolving steel counter circle is held against the wear test pins, which are made of composite materials and have dimensions of 10 mm in width and 30 mm in length. Between testing, the counter disc and the samples are meticulously cleaned to remove any worn material that may have adhered to the disc or sample. To make sure the level surface connected with the steel circle before testing, the surfaces of the pin tests were scrubbed against emery paper. The weight of the example is calculated using a computerized weighing offset with a high accuracy of 0.0001g after washing with the  $C_3H_6O$  solution. The weight loss is used to calculate the wear rate, which is expressed as wear volume loss per unit sliding distance [15].

### 2.2.3 Taguchi-Grey Relational Analysis

Using Taguchi's L27 experimental design, the friction and wear of manufactured AMMCs were measured following ASTM G-99 [16]. The ideal set of process parameters at which the friction and wear values become optimal was determined using the GRA approach with three process parameters; Load (N), distance (m), and speed (m/s). The levels of the process parameters are shown in Table 4.

Table 4. Selection of process parameters

| S. No | Material    | Load | Distance | Speed |
|-------|-------------|------|----------|-------|
| 1     | Al-6Gr-4SiC | 20   | 1000     | 1.5   |
| 2     | Al-4Gr-6SiC | 40   | 2000     | 3     |
| 3     | Al-6Gr-6SiC | 60   | 3000     | 4.5   |

## 3. Results and Discussion

### 3.1. Morphology of Fabricated Samples

The morphology of the manufactured samples, namely the aluminum stir-cast hybrid composites reinforced with silicon carbide and graphite particles, has a significant impact on their structural features and subsequent performance in different applications. SEM study of the base alloy (Al-6061) is shown in Figure 3(a), revealing the microstructure of the unaltered aluminum matrix. Figure 3(b) specifically examines the scanning electron microscopy (SEM) examination of Al-6Gr-4SiC samples, which shows a clear concentration of the reinforcing particles. The clustering seen may be ascribed to causes such as uneven distribution during the stirring process or inadequate dispersion of the graphite (Gr) and silicon carbide (SiC) particles inside the aluminum matrix. The observed clustering has the potential to affect the mechanical and tribological characteristics of the composite, hence impacting parameters like hardness and wear resistance.

The SEM examination of Al-4Gr-6SiC samples in Figure 3(c) reveals a surface that is much smoother in comparison to Figure 3(b). The enhanced smoothness of the Al-4Gr-6SiC samples may be ascribed to the enhanced dispersion and uniform distribution of the graphite and silicon carbide particles inside the aluminum matrix. The enhanced dispersion is probably due to the optimized processing settings used during the stir-casting process, resulting in a more homogeneous integration of the reinforcement phases. The SEM examination of Al-6Gr-6SiC samples, as shown in Figure 3(d), reveals a surface where reinforcement particles are evenly distributed throughout the aluminum matrix. The uniform dispersion seen in this picture is likely due to many variables that enhance the efficiency of processing and mixing during the stir-casting process.

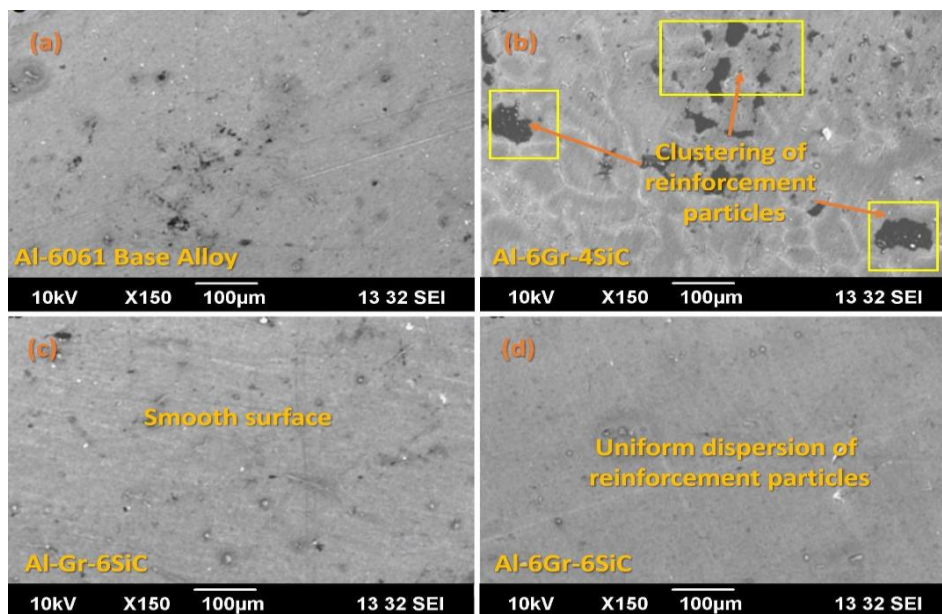


Fig. 3. Morphology of fabricated samples

### 3.2. Hardness and Tensile Strength

Hardness is a material property that measures its resistance to deformation, particularly when subjected to an indentation or applied load. The Vickers hardness test is a popular method that uses a diamond-shaped indenter. The hardness value is determined by measuring the diagonals of the resulting indentation. The Vickers Hardness Number (VHN) is calculated based on the applied force (200 gf) and the surface area of the indentation. Based on the hardness measurements the hardness value of the sample (Al-6Gr-4SiC) is measured to be 102 VHN. The hardness value of the sample (Al-4Gr-6SiC) is recorded as 116 VHN. The sample composed of aluminum, graphite, and silicon carbide (Al-6Gr-6SiC) has the maximum recorded hardness, with a value of 128 Vickers Hardness Number (VHN). As Table 5 indicates it is evident that the sample (Al-6Gr-6SiC) exhibits the highest level of hardness among the three samples. This finding indicates that, within the scope of this particular comparison, the composite denoted as "Al-6Gr-6SiC," which has a greater concentration of silicon carbide (SiC), exhibits the highest level of hardness among the materials subjected to testing. The heightened level of hardness may prove to be beneficial in scenarios where the ability to withstand wear and maintain hardness is of utmost importance, particularly in components that are exposed to abrasive environments.

Table 5. Mechanical properties of hybrid composites

| S. No | Samples     | Hardness (VHN) |      |      |      | Tensile Strength (MPa) |     |     |      |
|-------|-------------|----------------|------|------|------|------------------------|-----|-----|------|
|       |             | VHN1           | VHN2 | VHN3 | Mean | TS1                    | TS2 | TS3 | Mean |
| 1     | Al-6Gr-4SiC | 103            | 101  | 102  | 102  | 212                    | 216 | 214 | 214  |
| 2     | Al-4Gr-6SiC | 114            | 116  | 115  | 116  | 235                    | 239 | 237 | 237  |
| 3     | Al-6Gr-6SiC | 126            | 130  | 128  | 128  | 251                    | 253 | 255 | 253  |

In a similar vein, it can be seen that the sample (Al-6Gr-6SiC) exhibits the highest value of tensile strength when compared to the other two samples as shown in Figure 4 (a). This

finding indicates that, within the context of this particular comparison, the composite denoted as "Al-6Gr-6SiC," which has a greater concentration of silicon carbide (SiC), demonstrates the greatest level of tensile strength. The heightened tensile strength is beneficial in scenarios where materials must endure substantial stretching or pulling pressures without experiencing considerable deformation or fracture. This observation suggests that the composite material being referred to exhibits the highest level of strength when compared to the other materials that were evaluated within the given context. Figure 4 (a and b) shows the tensile test samples before and after testings.

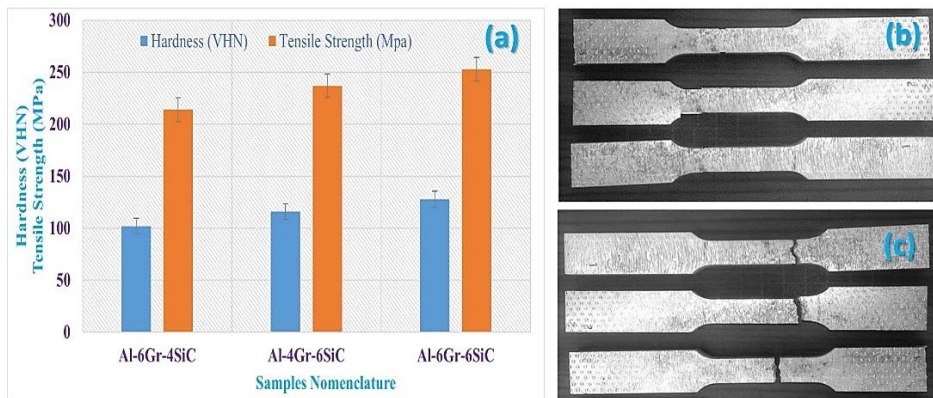


Fig. 4 Graphical representation of hardness and tensile strength

### 3.3. Wear and Friction Measurement

Sample No. 3 (Al-6Gr-6SiC) is selected for conducting the dry wear and friction tests due to its superior hardness and tensile strength compared to the other two samples. An increase in hardness generally signifies enhanced resistance to wear, whereas a higher tensile strength implies increased strength and endurance under applied stresses. The performance of Sample 3 is assessed in settings where friction and wear are significant variables by the implementation of dry wear and friction tests. This testing methodology has the potential to provide significant insights into the material's performance in practical scenarios, particularly when subjected to abrasive or sliding contact with various surfaces. The measured values of wear and friction are represented in Figure 5.

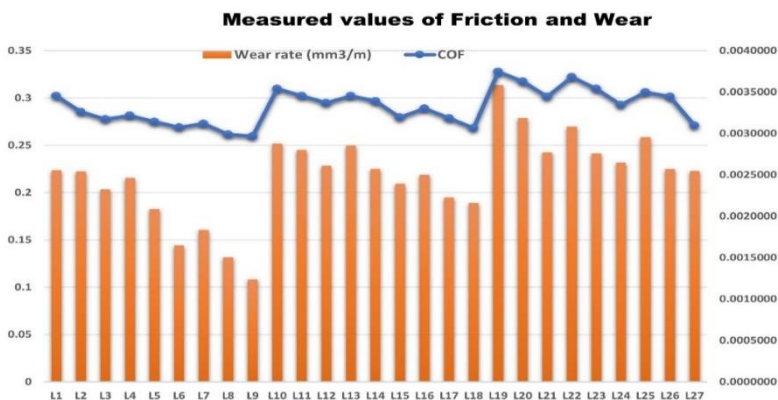


Fig. 5. Measured values for wear and friction

### 3.5. Optimization using the GRA Approach

Table 6 shows the orthogonal array with experimental observation after the wear test on the Pin-on-disc apparatus. In the grey relational analysis, the real several outputs were reduced to a single output. In this method, the final stage of grading was given to the output values as shown in Table 7. Getting the normalized values from the response data is the first stage in the procedure. The second stage involves calculating the departure from the sequence, and the third involves determining the grey relationship coefficient. The grey relational grades (GRG) are created in the next step by calculating the mean of the GR coefficient, and the highest rank is then used to determine the best combination of answer values [17]–[19].

Table 6. Orthogonal Array with experimental observation

| S. No | Orthogonal Array | Load (N) | Speed (m/s) | Distance (m) | COF    | Wear rate (mm <sup>3</sup> /m) |
|-------|------------------|----------|-------------|--------------|--------|--------------------------------|
| 1     | L <sub>1</sub>   | 20       | 1.5         | 1000         | 0.3023 | 0.0026                         |
| 2     | L <sub>2</sub>   | 20       | 1.5         | 2000         | 0.2852 | 0.0025                         |
| 3     | L <sub>3</sub>   | 20       | 1.5         | 3000         | 0.2776 | 0.0023                         |
| 4     | L <sub>4</sub>   | 20       | 3           | 1000         | 0.2814 | 0.0025                         |
| 5     | L <sub>5</sub>   | 20       | 3           | 2000         | 0.2748 | 0.0021                         |
| 6     | L <sub>6</sub>   | 20       | 3           | 3000         | 0.2691 | 0.0016                         |
| 7     | L <sub>7</sub>   | 20       | 4.5         | 1000         | 0.2729 | 0.0018                         |
| 8     | L <sub>8</sub>   | 20       | 4.5         | 2000         | 0.2615 | 0.0015                         |
| 9     | L <sub>9</sub>   | 20       | 4.5         | 3000         | 0.2596 | 0.0012                         |
| 10    | L <sub>10</sub>  | 40       | 1.5         | 1000         | 0.3098 | 0.0029                         |
| 11    | L <sub>11</sub>  | 40       | 1.5         | 2000         | 0.3023 | 0.0028                         |
| 12    | L <sub>12</sub>  | 40       | 1.5         | 3000         | 0.2947 | 0.0026                         |
| 13    | L <sub>13</sub>  | 40       | 3           | 1000         | 0.3023 | 0.0029                         |
| 14    | L <sub>14</sub>  | 40       | 3           | 2000         | 0.2966 | 0.0026                         |
| 15    | L <sub>15</sub>  | 40       | 3           | 3000         | 0.2795 | 0.0024                         |
| 16    | L <sub>16</sub>  | 40       | 4.5         | 1000         | 0.2890 | 0.0025                         |
| 17    | L <sub>17</sub>  | 40       | 4.5         | 2000         | 0.2786 | 0.0022                         |
| 18    | L <sub>18</sub>  | 40       | 4.5         | 3000         | 0.2681 | 0.0022                         |
| 19    | L <sub>19</sub>  | 60       | 1.5         | 1000         | 0.3278 | 0.0036                         |
| 20    | L <sub>20</sub>  | 60       | 1.5         | 2000         | 0.3174 | 0.0032                         |
| 21    | L <sub>21</sub>  | 60       | 1.5         | 3000         | 0.3013 | 0.0028                         |
| 22    | L <sub>22</sub>  | 60       | 3           | 1000         | 0.3222 | 0.0031                         |
| 23    | L <sub>23</sub>  | 60       | 3           | 2000         | 0.3098 | 0.0028                         |
| 24    | L <sub>24</sub>  | 60       | 3           | 3000         | 0.2928 | 0.0026                         |
| 25    | L <sub>25</sub>  | 60       | 4.5         | 1000         | 0.3060 | 0.0030                         |
| 26    | L <sub>26</sub>  | 60       | 4.5         | 2000         | 0.3013 | 0.0026                         |
| 27    | L <sub>27</sub>  | 60       | 4.5         | 3000         | 0.2710 | 0.0025                         |



Table 7. Grey relational analysis

| S. No | Normalized value |       | Deviation Sequence |       | GR Coefficient |       | GRG   | RANK |
|-------|------------------|-------|--------------------|-------|----------------|-------|-------|------|
| 1     | 0.625            | 0.560 | 0.375              | 0.440 | 0.571          | 0.532 | 0.552 | 10   |
| 2     | 0.375            | 0.554 | 0.625              | 0.446 | 0.444          | 0.529 | 0.487 | 16   |
| 3     | 0.264            | 0.462 | 0.736              | 0.538 | 0.404          | 0.482 | 0.443 | 20   |
| 4     | 0.319            | 0.519 | 0.681              | 0.481 | 0.424          | 0.510 | 0.467 | 17   |
| 5     | 0.222            | 0.361 | 0.778              | 0.639 | 0.391          | 0.439 | 0.415 | 22   |
| 6     | 0.139            | 0.174 | 0.861              | 0.826 | 0.367          | 0.377 | 0.372 | 25   |
| 7     | 0.194            | 0.254 | 0.806              | 0.746 | 0.383          | 0.401 | 0.392 | 24   |
| 8     | 0.028            | 0.114 | 0.972              | 0.886 | 0.340          | 0.361 | 0.350 | 26   |
| 9     | 0.000            | 0.000 | 1.000              | 1.000 | 0.333          | 0.333 | 0.333 | 27   |
| 10    | 0.736            | 0.695 | 0.264              | 0.305 | 0.655          | 0.621 | 0.638 | 4    |
| 11    | 0.625            | 0.664 | 0.375              | 0.336 | 0.571          | 0.598 | 0.585 | 8    |
| 12    | 0.514            | 0.583 | 0.486              | 0.417 | 0.507          | 0.545 | 0.526 | 13   |
| 13    | 0.625            | 0.687 | 0.375              | 0.313 | 0.571          | 0.615 | 0.593 | 7    |
| 14    | 0.542            | 0.566 | 0.458              | 0.434 | 0.522          | 0.535 | 0.529 | 12   |
| 15    | 0.292            | 0.490 | 0.708              | 0.510 | 0.414          | 0.495 | 0.454 | 18   |
| 16    | 0.431            | 0.535 | 0.569              | 0.465 | 0.468          | 0.518 | 0.493 | 15   |
| 17    | 0.278            | 0.421 | 0.722              | 0.579 | 0.409          | 0.463 | 0.436 | 21   |
| 18    | 0.125            | 0.392 | 0.875              | 0.608 | 0.364          | 0.451 | 0.407 | 23   |
| 19    | 1.000            | 0.997 | 0.000              | 0.003 | 1.000          | 0.993 | 0.997 | 1    |
| 20    | 0.847            | 0.828 | 0.153              | 0.172 | 0.766          | 0.744 | 0.755 | 3    |
| 21    | 0.611            | 0.651 | 0.389              | 0.349 | 0.562          | 0.589 | 0.576 | 9    |
| 22    | 0.917            | 0.784 | 0.083              | 0.216 | 0.857          | 0.698 | 0.778 | 2    |
| 23    | 0.736            | 0.646 | 0.264              | 0.354 | 0.655          | 0.586 | 0.620 | 6    |
| 24    | 0.486            | 0.599 | 0.514              | 0.401 | 0.493          | 0.555 | 0.524 | 14   |
| 25    | 0.681            | 0.729 | 0.319              | 0.271 | 0.610          | 0.649 | 0.629 | 5    |
| 26    | 0.611            | 0.566 | 0.389              | 0.434 | 0.563          | 0.535 | 0.549 | 11   |
| 27    | 0.167            | 0.556 | 0.833              | 0.444 | 0.375          | 0.530 | 0.452 | 19   |

3.5.1. ANOVA for GRG's

ANOVA was used to examine each process parameter's percentage contribution and its significance at a 95% confidence level [20]. The acquired findings of the GRGs' ANOVA are displayed in Table 6.

Table 8. Analysis of variance for GRG's

| Source       | DF | Adj SS   | Adj MS   | F-Value | P-Value |
|--------------|----|----------|----------|---------|---------|
| Load (N)     | 2  | 0.240204 | 0.120102 | 13.90   | 0.000   |
| Speed (m/s)  | 2  | 0.127637 | 0.063818 | 7.38    | 0.004   |
| Distance (m) | 2  | 0.006978 | 0.003489 | 0.40    | 0.673   |
| Error        | 20 | 0.172867 | 0.008643 |         |         |
| Total        | 26 | 0.547685 |          |         |         |

R<sup>2</sup> = 68.44% R<sup>2</sup>(adj) = 58.97 %

The findings indicated that load, distance, and sliding speed percentages contributed 61.505%, 25.124%, and 13.371%, respectively, to the ideal values of friction and wear [21]–[23]. According to Table 8, all of the criteria were found to be relevant. Figure 6 shows the residual plots for Grey Relational Grades.

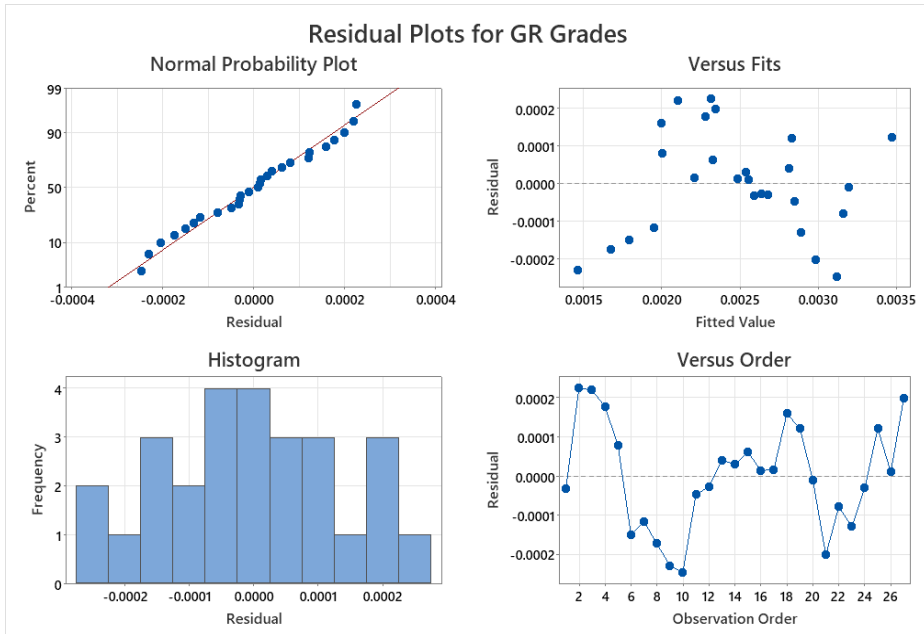


Fig. 6 Residual plots for Grey Relational Grades

### 3.5.2. Regression Equations

#### 3.5.2.1 Coefficient of Friction

0.290917 - 0.01488 Load (N)\_20 + 0.00028 Load (N)\_40 + 0.01460 Load (N)\_60 + 0.01112 Speed (m/s) 1.5 + 0.00112 Speed (m/s)\_3.0 - 0.01225 Speed (m/s)\_4.5 + 0.01060 Distance (m)\_1000 + 0.00102 Distance (m)\_2000 - 0.01162 Distance (m)\_3000 = 0.29776

#### 3.5.2.2 Wear Rate (mm<sup>3</sup>/m)

0.002492 - 0.000470 Load (N)\_20 + 0.000062 Load (N)\_40 + 0.000408 Load (N)\_60 + 0.000314 Speed (m/s)\_1.5 + 0.000008 Speed (m/s)\_3.0 - 0.000322 Speed (m/s)\_4.5 + 0.000253 Distance (m)\_1000 - 0.000020 Distance (m)\_2000 - 0.000233 Distance (m)\_3000 = 0.002588 mm<sup>3</sup>/m

Figure 7 represents the effect of wear testing parameters on wear rate. The function of load is major, accounting for a substantial portion (61.505%) of the observed variation in GRG. The high F-value (13.90) and low p-value (0.000) suggest that the load has a substantial impact on the friction and wear performance of the hybrid composites, making it a highly relevant factor. Variations in load levels have a significant influence on the results. Velocity is an additional crucial factor, making a substantial contribution (25.124%) to the total variation in GRG. The F-value of 7.38 and the p-value of 0.004 indicate the statistical importance of speed. Changes in the speed at which objects slide against one another have an impact on their frictional behavior, highlighting the significance of speed in attaining the best possible performance. Distance, while it contributes to the variation (13.371%), has a lesser influence in comparison to load and speed. The F-value of 0.40 and the p-value of 0.673 indicate that distance has a relatively weak statistical significance in impacting

GRG. Variations in the distance of sliding have a relatively lesser effect on the observed tribological results. The aggregate impact of load, speed, and distance explains a significant proportion (about 68.44%) of the observed variation in GRG. The small p-values for load and speed show a strong degree of confidence in their importance, confirming their essential roles in attaining ideal tribological features. Distance, while it has an impact, is statistically less important in the context of this research.

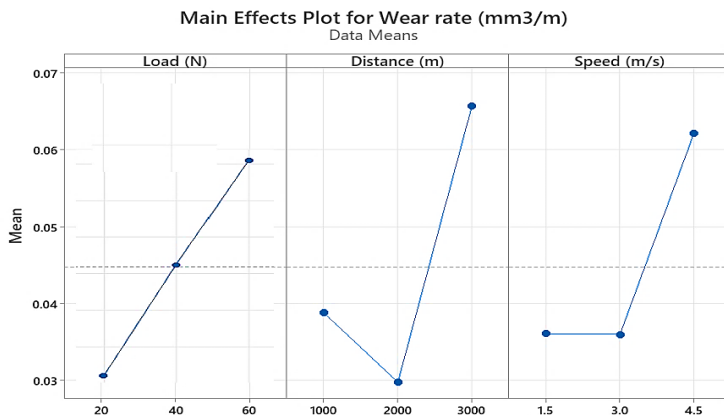


Fig. 7. Effect of process parameters on wear rate

### 3.6. Micrographs of Worn-Out Surfaces After Wear Test

The friction and wear of the synthesized hybrid AMMCs supplemented with graphene and silicon carbide particles are depicted in Figure 5 [24]–[26]. After the inclusion of hard reinforcement particles and their uniform dispersion in the matrix material, an increase in friction and a decrease in wear rate were noted [27]–[29]. The examination of sliding wear behavior included a comprehensive analysis under different situations, with specific attention given to worn surfaces using scanning electron microscope observations. Out of all the factors that were evaluated, the applied load was shown to be the most relevant influence on wear rate. As a result, worn-out surfaces were examined while being subjected to applied stresses of 20 N, 40 N, and 60 N.

Distinct characteristics, including peeled-off particles, delamination, and abrasive wear, were seen at a load of 20 N (Figure 8a) [30]–[32]. The impact intensified when subjected to a 40 N force (Figure 8b), exposing features such as oxidation and adhesive wear. At 60 N load, there was clear evidence of delamination and the appearance of tiny particles (Figure 8c) [33]–[35]. The inclusion of cerium oxide particles significantly improved the hardness and wear resistance of the produced specimens. Nevertheless, an increase in the hardness of the surfaces in contact resulted in the deterioration and wearing away of the material. Sliding wear may lead to the formation of a heterogeneous dispersion layer, which in turn produces debris consisting of particles of aluminum, iron, carbon, and silicon oxide. The inclusion of planar surfaces and increased rigidity, caused by plastic deformation, led to a reduction in the wear rate of the composites. The observation shows that the lowest wear rate of 0.002588 mm<sup>3</sup>/N-m when subjected to a 60 N load, sliding over a distance of 1000 m, and at a velocity of 1.5 m/s.

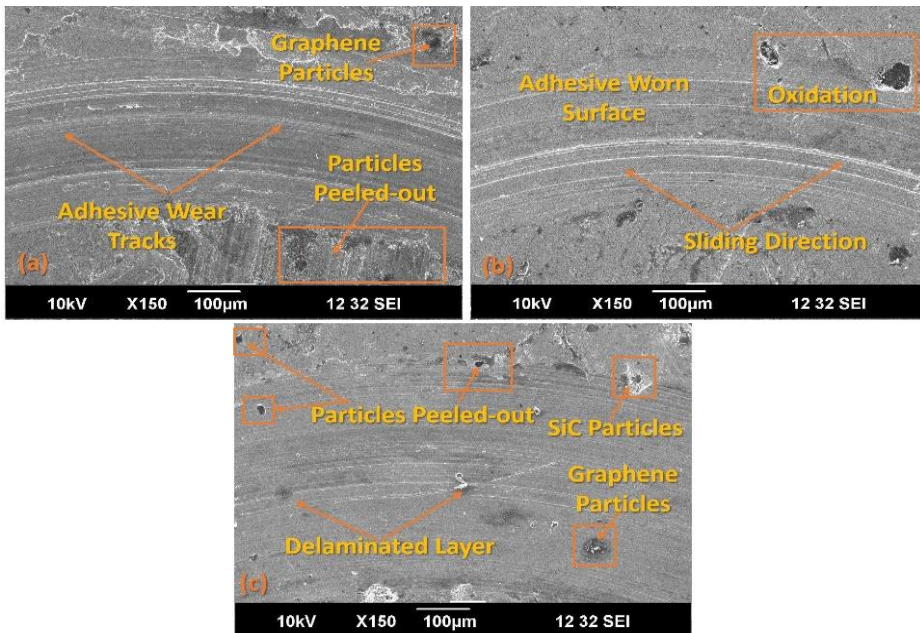


Fig. 8. (a, b, and c) SEM Morphology of Worn-out surfaces after Wear test

#### 4. Conclusions

The main aim of the current study was to find the optimized set of stir-casting parameters using grey relational analysis, which simultaneously affects the friction and wear of the fabricated AMMCs. The conclusions of the study are mentioned below:

- The research effectively optimized the fabrication parameters for hybrid aluminum metal matrix composites (AMMCs) by using grey relational analysis (GRA) and Taguchi's  $L_{27}$  design.
- The Al-6Gr-6SiC composite proved to be the most favorable combination, demonstrating exceptional hardness (measured at 128 Vickers Hardness Number) and tensile strength (measured at 253 MPa).
- The use of both graphene (Gr) and silicon carbide (SiC) as reinforcements in the Al-6061 matrix resulted in enhanced tribological characteristics of the hybrid AMMCs.
- The chosen composite exhibited improved resistance to friction, with a coefficient of friction of 0.29766, and reduced wear rates, measuring  $0.002588 \text{ mm}^3/\text{m}$ .
- The tribological behavior of AMMCs is significantly influenced by the parameters of load, sliding speed, and sliding distance. The research highlighted the crucial roles they play in attaining ideal mechanical and frictional characteristics.
- The analysis of variance (ANOVA) findings highlighted the significant impacts of load (61.505%), speed (25.124%), and distance (13.371%) on achieving optimal friction and wear values.
- Analysis using scanning electron microscopy (SEM) of the manufactured samples showed clear microstructural traits that have an impact on the mechanical and tribological properties.
- The arrangement and spread of reinforcing particles were seen to influence hardness, resistance to wear, and the overall performance of the composite.
- The optimized composite (Al-6Gr-6SiC) shows promise for use in applications that need exceptional wear resistance and durability.

## Acknowledgment

The authors acknowledge that this study is supported by the National Institute of Technology Kurukshetra, India.

## References

- [1] Jawalkar CS, Singh A, Suri NM. Fabrication of Aluminium Metal Matrix Composites with Particulate Reinforcement : A Review. *Materials Today: Proceedings*. 2017;4(2):2927-2936. <https://doi.org/10.1016/j.matpr.2017.02.174>
- [2] Samal BP, Khuntia SK. Corrosion Behavior of Al-Mg-SiC Composite produced by Modified Stir casting method. 2019;14(12):2821-2823.
- [3] Kumar D, Singh S, Angra S. Dry sliding wear and microstructural behavior of stir-cast Al6061-based composite reinforced with cerium oxide and graphene nanoplatelets. *Wear*. 2023;516-517:204615. <https://doi.org/10.1016/j.wear.2022.204615>
- [4] Kumar H, Kumar V, Kumar D, Singh S. Wear Behavior of Friction Stir Processed Copper-Cerium Oxide Surface Composites. *EVERGREEN Joint Journal of Novel Carbon Resource Sciences & Green Asia Strategy*. 2023;10(01):78-84. <https://doi.org/10.5109/6781043>
- [5] Chowdhury MA, Kumar UD, Kchaou M, Shuvho BA, Rahman A, Kumar BR. Correlation between experimental and analytic approaches to study the erosion rate of aluminum-metal matrix composites. *Journal of Engineering Research (Kuwait)*. 2022;10(1):295-315
- [6] Engineering M, Kavary T, Nadu ST. Tribological And Corrosion Behaviour Of Al 6063 / SiC Metal Matrix Composites. *International Journal of Advanced Engineering Technology*, VII(II), 2016;2-7.
- [7] Hashim FA, Abdulkader NJ. Corrosion Behavior of Recycling Al- Alloy Based Metal Matrix Composites Reinforced by Nano particles. *Kurdistan Journal of Applied Research*. 2017; 2(3): 279-283.
- [8] Saravanan C, et al. Investigation on the mechanical, tribological, morphological and machinability behavior of stir-casted Al/SiC/Mo reinforced MMCs. *Materials Today: Proceedings*. 2020;21:1-10.
- [9] Mercado-Lemus VH, et al. Wear Dry Behavior of the Al-6061-Al2O3 Composite Synthesized by Mechanical Alloying. *Metals*. 2021;1-17. <https://doi.org/10.3390/met11101652>
- [10] C Mk. Effect of Carbon Nanotube in Aluminum Metal Matrix Composites on Mechanical Properties. *Journal of Engineering Science and Technology* 2020;15(2):919-930.
- [11] Wei L, Liu X, Gao Y, Lv X, Hu N, Chen M. Synergistic strengthening effect of titanium matrix composites reinforced by graphene oxide and carbon nanotubes. *Materials and Design*. 2021;197:109261. <https://doi.org/10.1016/j.matdes.2020.109261>
- [12] Suresh R. Comparative study on dry sliding wear behavior of mono (Al2219 / B 4 C ) and hybrid ( Al2219 / B 4 C / Gr ) metal matrix composites using statistical technique. *Journal of the Mechanical Behavior of Materials* 2020;57-68. <https://doi.org/10.1515/jmbm-2020-0006>
- [13] Kumar D, Angra S, Singh S. Effect of reinforcements on mechanical and tribological behavior of magnesium-based composites : a review. *Material Physics and Mechanics* 2022;50(3):439-458.
- [14] Kumar D, Angra S, Singh S. High-temperature dry sliding wear behavior of hybrid aluminum composite reinforced with ceria and graphene nanoparticles. *Engg Failure Analysis*,2023;151(May):107426. <https://doi.org/10.1016/j.engfailanal.2023.107426>
- [15] Sharma VK, Kumar V, Joshi RS. Experimental investigation on effect of RE oxides addition on tribological and mechanical properties of Al-6063 based hybrid composites Experimental investigation on effect of RE oxides addition on tribological and

- mechanical properties of Al-6063 based hybrid composites. *Materials Research Express* 2019; Vol. 6, PP.1-18, <https://doi.org/10.1088/2053-1591/ab2504>
- [16] Ravichandran G, Rathnakar G, Santhosh N, Suresh R. Wear characterization of hnt filled glass-epoxy composites using taguchi's design of experiments and study of wear morphology. *Composites Theory and Practice*. 2020;20(2):85-91.
- [17] Khatkar SK, Verma R, Kharb SS, Thakur A, Sharma R. Optimization and Effect of Reinforcements on the Sliding Wear Behavior of Self-Lubricating AZ91D-SiC-Gr Hybrid Composites. *Silicon*, 2021;1461-1473. <https://doi.org/10.1007/s12633-020-00523-0>
- [18] Vedabouriswaran G, Aravindan S. Wear Characteristics of Friction Stir Processed Magnesium RZ 5 Composites. *Journal of Tribology*. 2019;141(4). <https://doi.org/10.1115/1.4042039>
- [19] Kumar A, Arafath Y, Gupta P, Kumar D, Mustansar C, Jamwal A. Materials Today: Proceedings Microstructural and mechano-tribological behavior of Al reinforced SiC-TiC hybrid metal matrix composite. *Materials Today: Proceedings*. 2019;8-11. <https://doi.org/10.1016/j.matpr.2019.08.186>
- [20] Begum Y, Bharath KN, Doddamani S, Rajesh AM, Kaleemulla KM. Optimization of Process Parameters of Fracture Toughness Using Simulation Technique Considering Aluminum-Graphite Composites. *Transactions of the Indian Institute of Metals*. 2020;73(12):3095-3103. <https://doi.org/10.1007/s12666-020-02113-5>
- [21] Okumus M. Study of microstructural, mechanical, thermal and tribological properties of graphene oxide reinforced Al - 10Ni metal matrix composites prepared by mechanical alloying method. *Wear* 2022;511(September). <https://doi.org/10.2139/ssrn.4082693>
- [22] Hamada ML, Alwan GS, Annaz AA, Irbhayim SS, Hammood HS. Experimental Investigation of Mechanical and Tribological Characteristics of Al 2024 Matrix Composite Reinforced by Yttrium Oxide Particles. *Korean Journal of Material Research* 2021;31(6):339-344. <https://doi.org/10.3740/MRSK.2021.31.6.339>
- [23] Al MMA, Allam QIM, Patel F, Samad A. Tribological Performance of Sub - Micron - Al 2 O 3 - Reinforced Aluminum Composite Brake Rotor Material. *Arabian Journal for Science and Engineering*. 2021;46(3):2691-2700. <https://doi.org/10.1007/s13369-020-05179-x>
- [24] Chak V, Chattopadhyay H, Dora TL. A review on fabrication methods, reinforcements and mechanical properties of aluminum matrix composites. *Journal of Manufacturing Processes*. 2020;56(May):1059-1074. <https://doi.org/10.1016/j.jmapro.2020.05.042>
- [25] Ramadoss N, Pazhanivel K, Ganesh Kumar S, Arivanandhan M, Anandan P. Effect of B4C and SiC nanoparticle reinforcement on the wear behavior and surface structure of aluminum (Al6063-T6) matrix composite. *SN Applied Sciences*. 2020;2(5):1-16. <https://doi.org/10.1007/s42452-020-2712-5>
- [26] Nyadongo ST. Analysis of Dry Sliding Wear Performance of Tribaloy T-800 / Tungsten Carbide Coating Deposited via Laser Cladding Assisted with Preheating. *Journal of Materials Engineering and Performance*. 2022; 32(12), 5435-5449. <https://doi.org/10.1007/s11665-022-07493-x>
- [27] Kumar D, Angra S, Singh S. Mechanical Properties and Wear Behaviour of Stir Cast Aluminum Metal Matrix Composite: A Review. *International Journal of Engineering, Transactions A: Basics*. 2022;35(4):794-801. <https://doi.org/10.5829/IJE.2022.35.04A.19>
- [28] Vageshappa LS, Channabasappa M. Effect of addition of TiC nanoparticles on the tensile strength of Al7075-graphene hybrid composites *Research on Engineering Structures and Materials*, 9(1), 19-30, 2023. <https://doi.org/10.17515/resm2022.486ma0725>
- [29] Singh C, Kumar V, Manna A. Experimental study on developed electrochemical micro machining of hybrid MMC. *Indian Journal of Engineering & Materials Sciences* 2020;27(June):579-589. <https://doi.org/10.56042/ijems.v27i3.45055>

- [30] Khan MM, Dey A, Hajam MI. Experimental Investigation and Optimization of Dry Sliding Wear Test Parameters of Aluminum Based Composites. *Silicon* 2022;4009-4026. <https://doi.org/10.1007/s12633-021-01158-5>
- [31] Jagannatham M, Saravanan MSS, Sivaprasad K, Babu SPK. Mechanical and Tribological Behavior of Multiwalled Carbon Nanotubes-Reinforced AA7075 Composites Prepared by Powder Metallurgy and Hot Extrusion. *Journal of Materials Engineering and Performance*. 2018;27(11):5675-5688. <https://doi.org/10.1007/s11665-018-3681-3>
- [32] Bhoi NK, Singh H, Pratap S. Developments in the aluminum metal matrix composites reinforced by micro / nano particles - A review. *Journal of Composite Materials* 2019. <https://doi.org/10.1177/0021998319865307>
- [33] Singh S, Pal K. Influence of Texture Evolution on Mechanical and Damping Properties of SiC/Li<sub>2</sub>ZrO<sub>3</sub>/Al Composite through Friction Stir Processing. *Journal of Engineering Materials and Technology, Transactions of the ASME*. 2020;142(2):1-9. <https://doi.org/10.1115/1.4045495>
- [34] Kubit A. The Effect of Adhesive Type on Strength of Inter-Layer Joints in Fiber Metal Laminate Composites. *Composites Theory and Practice*. 2017;17(3):162-168.
- [35] Ra'ayatpour M, Emamy M, Rassizadehghani J. Influence of Hot Extrusion on the Microstructure, Tensile and Wear Properties of Mg-5Sb-xSiC Hybrid Composites. *Metals and Materials International*. 2021; 28(3), 679-694. <https://doi.org/10.1007/s12540-020-00936-x>